A First All-Particle Cosmic Ray Energy Spectrum From IceTop

Fabian Kislat*, Stefan Klepser†, Hermann Kolanoski‡ and Tilo Waldenmaier‡
for the IceCube Collaboration*

*DESY, D-15738 Zeuthen, Germany
†IFAE Edifici Cn., Campus UAB, E-08193 Bellaterra, Spain
‡Institut für Physik, Humboldt-Universität zu Berlin, D-12489 Berlin, Germany
*See special section of these proceedings

***Abstract*. The IceTop air shower array is presently under construction at the geographic South Pole as part of the IceCube Observatory. It will consist of 80 stations which are pairs of Ice-Cherenkov tanks covering an area of $1\,\mathrm{km}^2$. In this paper a first analysis of the cosmic ray energy spectrum in the range $2 \cdot 10^{15}\,\mathrm{eV}$ to $10^{17}\,\mathrm{eV}$ is presented using data taken in 2007 with 26 IceTop stations. The all-particle spectrum has been derived by unfolding the raw spectrum using response matrices for different mass compositions of the primaries. Exploiting the zenith angle dependence of the air shower development we have been able to constrain the range of possible composition models.**

***Keywords*: IceTop - Energy - Spectrum**

I. Introduction

The IceTop air shower array is currently under construction as part of the IceCube Observatory at the geographic South Pole [1], [2]. Its 80 detector stations will cover an area of about $1\,\mathrm{km}^2$ at an atmospheric depth of $680\,\mathrm{g/cm}^2$. Each station consists of two ice filled $1.8\,\mathrm{m}$ diameter tanks each equipped with two Digital Optical Modules (DOMs) [3] as photon sensors (the same as used by IceCube in the deep ice). The photomultipliers inside the two DOMs are operated at different gains to increase the dynamic range.

Air showers are detected via the Cherenkov light emitted by charged particles inside the ice tanks. The light intensity is recorded by an 'Analog Transient Waveform Digitizer' (ATWD) at a $300\,\mathrm{MSPS}$ sampling rate. When the signal inside a DOM crosses a threshold a 'local coincidence' signal is sent to neigbouring DOMs. Data taking is started when a local coincidence signal is received from the high gain DOM in the other tank of a station within $250\,\mathrm{ns}$. This ensures that the two tanks of a station always trigger together. This analysis only uses events where at least five stations have triggered.

The analysis uses the signal sizes, obtained by integrating the waveforms, and the arrival times, determined from the leading edge of a waveform. Because of its high altitude of $2835\,\mathrm{m}$, IceTop is located close to the shower maximum for showers of energies between $10^{15}\,\mathrm{eV}$ and $10^{17}\,\mathrm{eV}$ (about $550\,\mathrm{g/cm}^2$ to $720\,\mathrm{g/cm}^2$). Therefore, the signals measured by IceTop are dominated by the electromagnetic component of the air showers.

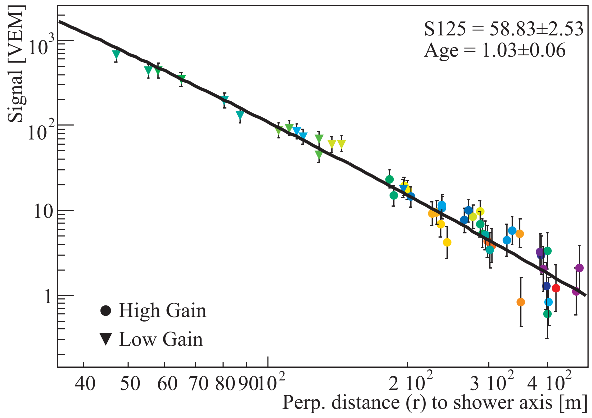

Fig. 1. An example of a lateral signal size distribution from a single event in IceTop. Each data point corresponds to the signal in terms of Vertical Equivalent Muons measured in an IceTop tank. The curve is a fit of the lateral distribution function (1).

II. Energy reconstruction

Generally, the shower direction can be reconstructed from the arrival times of signals, while the core position and the primary energy of the air shower are inferred from the lateral distribution of signal sizes. These signal sizes are calibrated with signals from vertical muons to eliminate differences between the tanks. Signals given in units of Vertical Equivalent Muons (VEM) are a detector independent measure of the intensity of an air shower at the position of a tank.

A first estimate of the shower core position is obtained by finding the signal center-of-gravity which is defined as the average of the tank positions weighted by the square-root of the signal size. The shower direction is obtained by fitting a plane to the measured signal times. These two first guesses are used as an input to a more accurate iterative maximum likelihood fit.

In the latter procedure a lateral distribution function is fitted to the measured signal sizes and an arrival time distribution is fitted to the signal times. The lateral distribution function [4] has been obtained from air shower and detector simulations and corresponds to a second order polynomial on a double logarithmic scale:

$$S(r) = S_{\mathrm{ref}} \left(\frac{r}{R_{\mathrm{ref}}} \right)^{-\beta_{\mathrm{ref}} - \kappa \log_{10}(r/R_{\mathrm{ref}})} \tag{1}$$

$S_{\rm ref}$ is the signal expectation value at the reference radius $R_{\rm ref}$ from the shower axis, $\beta_{\rm ref}$ is a slope parameter related to the shower age and κ is a curvature parameter of the lateral signal distribution function. Based on a study of the stability of fit results the reference radius has been fixed to $R_{\rm ref} = 125\,{\rm m}$ which also corresponds to the IceTop grid spacing. An example is shown in Figure 1. The likelihood function used in the fitting procedure is based on a study of signal fluctuations and also takes into account stations that do not trigger [4]. Taking into account the spatial curvature of the shower front, which is assumed to have a fixed profile [5], the arrival time distribution $t(r)$ is given by:

$$t(r) = 19.41\,{\rm ns}\left(e^{-\left(\frac{r}{118.1\,{\rm m}}\right)^2} - 1\right) - 4.823 \cdot 10^{-4}\frac{\rm ns}{\rm m^2}\,r^2 \qquad (2)$$

This $t(r)$ indicates the time delay of a signal at distance r from the shower axis with respect to a planar shower front through the shower core and perpendicular to the shower axis. Using this shower front parametrisation improves the direction resolution compared to the plane fit first guess result.

The complete log-likelihood function, therefore, has three terms,

$$L = L_{\rm hit} + L_{\rm nohit} + L_{\rm time} \qquad (3)$$

$L_{\rm hit}$ is based on the log-normal distribution of signal sizes obtained from the study of signal size fluctuations, $L_{\rm time}$ is based on an assumed Gaussian distribution of arrival times and $L_{\rm nohit}$ is defined by

$$L_{\rm nohit} = \sum \log\left(1 - P^A_{\rm hit} P^B_{\rm hit}\right) \qquad (4)$$

$P^i_{\rm hit}$ is the probability that tank i of a station triggers given the signal expectation of the fit at that iteration step, given the shower core position and direction. The likelihood accounts for the 'local coincidence' condition which requires both tanks of a station to trigger before signals are transmitted. The sum in (4) runs over all stations that did not trigger.

The fit procedure is divided into several steps to improve the stability. At first the direction is fixed to the initial first guess value and only the lateral signal distribution (1) is fitted. In a second iteration the direction is also varied but the parameters of the lateral fit are limited to a $\pm 3\sigma$ range around the values obtained in the first step. Finally a last iteration with fixed direction is performed. The slope parameter of the lateral distribution function is limited throughout this procedure to $1.5 \leq \beta_{125} \leq 5$.

Using the results of the fit a first-guess energy is determined as a function of shower size and the zenith angle. As a measure of the shower size, the signal expectation value $S_{\langle \log r \rangle}$, at the distance $\langle \log r \rangle$ from the core is used, where $\langle \log r \rangle$ is the average of the logarithmic distance of tanks to the shower axis. The size parameter $S_{\langle \log r \rangle}$ has been found to be least correlated to the other fit parameters (in general S_{125} and the slope β_{125} are correlated). From air shower simulations an energy estimator $E_{\rm rec}(S_{\langle \log r \rangle}, \theta)$ for any given $\langle \log r \rangle$ based on a proton hypothesis has been derived.

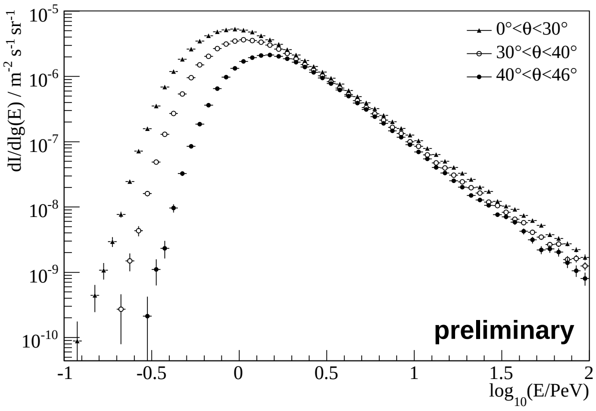

Fig. 2. Raw IceTop energy spectrum divided into three different zenith angle ranges (see text for details).

To ensure the quality of the reconstructed data several quality criteria are applied:

- Only showers with a zenith angle $\theta < 46°$ are considered restricting the analysis to a well understood zenith angle range;
- The value of the slope parameter must be $1.55 \leq \beta_{125} < 4.95$ removing all showers for which the likelihood fit ran into the limits on this parameter;
- The uncertainty on the shower core position must be less than $20\,{\rm m}$;
- The core position from the likelihood fit and the center-of-gravity first guess must be inside the IceTop array, $50\,{\rm m}$ away from the array border. Furthermore, the station with the largest signal must not be on the border of the IceTop array.

The last item is to exclude showers with a core outside the array which have a high probability to be misreconstructed. Using the likelihood fit result alone is not sufficient because the fit tends to reconstruct these cores inside the array. These strict requirements on the core reconstruction are necessary because the position of the core directly influences the interpretation of the fitted lateral distribution. Data was taken between June 1st 2007 and October 31st 2007 with the 26 IceTop stations operated at that time. The filter level data sample contained 11 262 511 events. After all of the above cuts, 4 131 343 events remained.

The raw energy spectrum, that is the distribution of the reconstructed energies $E_{\rm rec}$ without any further corrections or unfolding applied, but after the abovementioned cuts, is shown in Figure 2. The data is split into three zenith angle ranges, $0 \leq \theta < 30°$, $30° \leq \theta < 40°$ and $40° \leq 46°$.

III. AIR SHOWER SIMULATIONS

The relation between the measured signals and the properties of the primary particle can only be obtained

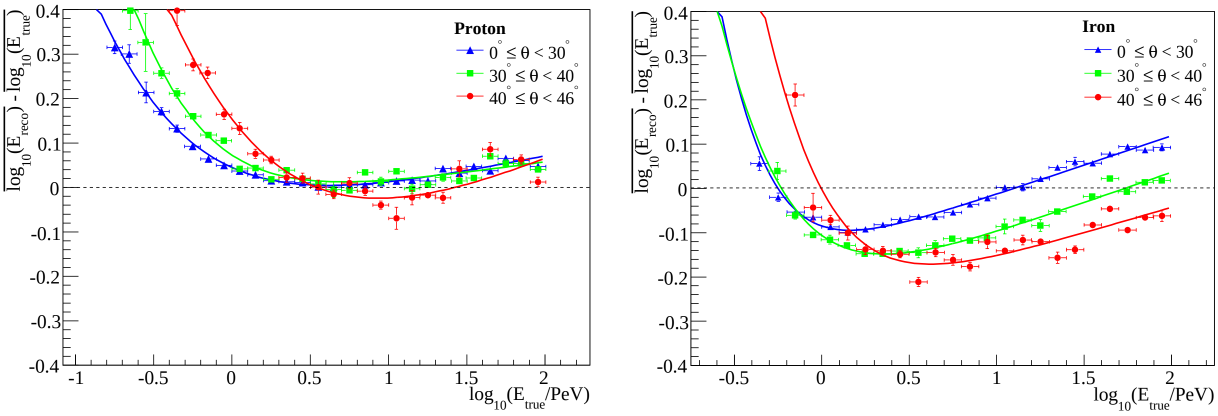

(a) Primary protons (b) Primary iron

Fig. 3. Systematic energy shift for (a) protons and (b) iron when using the energy estimator E_{rec} as a function of the true energy of a particle. This energy mis-reconstruction is one of the parameters describing the energy response of the IceTop detector. The strong increase towards low primary energies is a threshold effect as explained in the text. Since E_{rec} is based on the proton assumption the energy mis-reconstruction for protons is small while that for primary iron larger and shows a clear zenith angle dependance.

from simulations of air showers and the detector. Therefore, a Monte Carlo shower library containing 98 760 proton and iron showers with primary energies between $100\,\mathrm{TeV}$ and $100\,\mathrm{PeV}$ has been generated with CORSIKA [6]. The hadronic interaction models SIBYLL [7] and Fluka 2006.3b [8] and the CORSIKA atmosphere model No. 14 (South Pole, Dec. 31, 1997, MSIS-90-E) were used.

IV. Unfolding the spectrum

The energy estimator E_{rec} does not fully account for the angular and energy dependence of the detector acceptance and smearing. This biases the result especially in the threshold region where the detection efficiency increases strongly with energy. In addition, the calculation of E_{rec} assumes proton primaries and one specific atmosphere profile (CORSIKA atmosphere 12, South Pole July 01, 1997). A different atmosphere profile or a different composition of primary particles can result in a different energy spectrum. All these effects can be taken into account by unfolding the raw energy spectrum.

The unfolding algorithm uses a response matrix which contains the probability that an incident primary particle with true energy E_{true} will be assigned the energy E_{rec}. Response matrices are generated from CORSIKA air shower simulations for proton and iron primaries in three different zenith angle ranges. Response matrices for mixed compositions are obtained as linear combinations of these single primary particle responses.

To calculate the response matrices the simulated data are subdivided into 30 bins of true primary energies, equidistant in $\log_{10}(E_{\mathrm{true}})$. For each bin the energy response is obtained from a distribution of $\log_{10}(E_{\mathrm{rec}}/E_{\mathrm{true}})$ of all reconstructed events which is approximately normally distributed. Non-zero values of this quantity indicate a wrong energy reconstruction. As such the mean of this distribution is the 'energy mis-reconstruction', the width is the energy resolution. The reconstruction efficiency is the ratio between the number of reconstructed and generated events.

Depending on the zenith angle, the IceTop detector gets fully efficient at about $2\,\mathrm{PeV}$ with an effective area of $0.096\,\mathrm{km}^2$. The energy resolution improves with increasing energy and reaches a value of 0.05 in logarithm of energy at $10\,\mathrm{PeV}$ primary energy which corresponds to a statistical uncertainty of roughly $12\,\%$.

An important property of the detector response is the 'energy mis-reconstruction' shown in Figure 3. It is the systematic difference between the true primary energy and the reconstructed energy. The energy mis-reconstruction shows a strong dependence on the primary particle mass and thus on the assumed primary composition. The attenuation of iron induced showers with increasing slant depth is greater than for proton showers. This leads to an underestimation of the primary energy for inclined iron showers when using the proton-based energy estimator E_{rec}. This is nicely visible in Figure 3b.

V. Preliminary energy spectrum from IceTop

Based on these response matrices the three raw energy spectra of Figure 2 are unfolded using an iterative unfolding method [9]. An unfolding based on three different composition assumptions has been made: pure proton, pure iron and the two-component model consisting of proton and iron primaries as motivated in [10].

The results are shown in Figure 4. Above $4\,\mathrm{PeV}$ the spectra have a spectral index ranging from 2.93 to 3.19, depending on the composition assumption and the zenith angle band. The absolute normalization varies between $3.77 \cdot 10^{-15}\,\mathrm{m}^{-2}\mathrm{s}^{-1}\mathrm{sr}^{-1}\mathrm{GeV}^{-1}$ and $7.93 \cdot 10^{-15}\,\mathrm{m}^{-2}\mathrm{s}^{-1}\mathrm{sr}^{-1}\mathrm{GeV}^{-1}$ at an energy of $10\,\mathrm{PeV}$.

The abovementioned mis-reconstruction of the energy of inclined iron showers leads to a relative shift of the

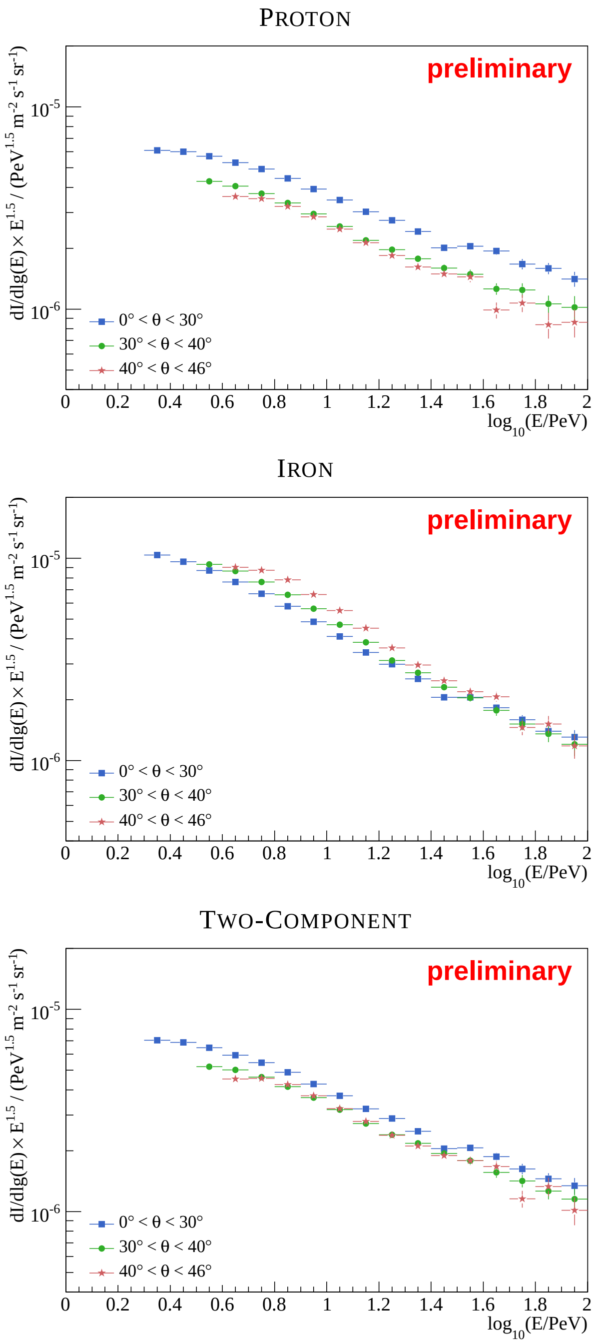

Fig. 4. Unfolding result for three different assumptions on the primary compositions: pure protons, pure iron, two-component model [10].

spectra from different zenith bands in the unfolding. In case of proton primaries the spectrum from the most vertical zenith bin shows the largest flux and the spectrum from the $40°$ to $46°$ zenith band shows the lowest flux. This order is reversed if the primary particles are assumed to be purely iron. Since there are no indications of an anisotropy of the arrival directions of cosmic rays in the energy range under consideration, isotropy has to be assumed. An isotropic flux, however, means that the unfolded spectra obtained from different zenith bands must agree.

VI. CONCLUSIONS AND OUTLOOK

A first analysis of the energy spectrum of cosmic rays in the range between $2\,\mathrm{PeV}$ and $100\,\mathrm{PeV}$ has been presented. This analysis uses an unfolding procedure to account for detector and atmospheric influences as well as differences in the shower development of different primary particles. Energy spectra have been obtained for three different compositions and three different zenith angle ranges. In case of a pure proton or iron hypothesis the three different inclination spectra do not agree which is in conflict with the assumption of an isotropic flux. Therefore those two pure composition assumptions can be excluded.

Several issues have not yet been addressed in this early study. Most importantly, the systematic uncertainties due to the interaction models used in the simulations must be studied. Also the influence of different atmosphere parametrisations in the simulation must be analysed and understood. This becomes even more important when analysing data from a longer period of time. Currently, in 2009, the detector is running with nearly three quarters of the full detector.

REFERENCES

[1] T.K. Gaisser *et al.* *IceTop: The Surface Component of IceCube*, in *Proc. 28th ICRC*, Tsukuba, Japan, 2003.
[2] T.K. Gaisser *et al.* *Performance of the IceTop Array*, in *Proc. 30th ICRC*, Mérida, Mexico, 2007; arXiv:0711.0353v1.
[3] R. Abbasi *et al.* "The IceCube Data Acquisition System: Signal Capture, Digitization, and Timestamping," Nucl. Instrum. Meth. A **601**, 294 (2009).
[4] S. Klepser *et al.* *Lateral Distribution of Air Shower Signals and Initial Energy Spectrum above 1 PeV from IceTop*, in *Proc. 30th ICRC*, Mérida, Mexico, 2007; arXiv:0711.0353v1.
[5] S. Klepser *et al.* *First Results from the IceTop Air Shower Array*, in *Proc. 21st ECRS*, Košice, Slovakia, 2008; arXiv:0811.1671v1.
[6] D. Heck *et al.*, Report **FZKA 6019** (1998), Forschungszentrum Karlsruhe; http://www-ik.fzk.de/corsika/physics_description/corsika_phys.html
[7] R. Engel, T.K. Gaisser, P. Lipari, and T. Stanev, *Air shower calculations with the new version of SIBYLL*, in *Proc. 26th ICRC*, Salt Lake City, USA, 1999.
[8] A. Ferrari, P.R. Sala, A. Fassò, and J. Ranft, "FLUKA: a multi-particle transport code", CERN-2005-10 (2005), INFN/TC 05/11, SLAC-R-773.
[9] G. D'Agostini, "A multidimensional unfolding method based on Bayes' theorem," Nucl. Instrum. Meth. A **362**, 487 (1995)
[10] R. Glasstetter *et al.* *Analysis of electron and muon size spectra of EAS*, in *Proc. 26th ICRC*, Salt Lake City, USA, 1999.
[11] S. Klepser, "Reconstruction of Extensive Air Showers and Measurement of the Cosmic Ray Energy Spectrum in the Range of $1-80\,\mathrm{PeV}$ at the South Pole", Dissertation, Humboldt-Universität zu Berlin, 2008.